

# Phase Transitions for Optimality Gaps in Optimal Power Flows

## A Study on the French Transmission Network

Terrence W.K. Mak, Lyndon Shi, Pascal Van Hentenryck

**Abstract**—This paper investigates phase transitions on the optimality gaps in Optimal Power Flow (OPF) problem on real-world power transmission systems operated in France. The experimental results study optimal power flow solutions for more than 6000 scenarios on the networks with various load profiles, voltage feasibility regions, and generation capabilities. The results show that bifurcations between primal solutions and the QC, SOCP, and SDP relaxation techniques frequently occur when approaching congestion points. Moreover, the results demonstrate the existence of multiple bifurcations for certain scenarios when load demands are increased uniformly. Preliminary analysis on these bifurcations were performed.

### I. INTRODUCTION

The AC Optimal Power Flow (AC-OPF) is an important and challenging problem in power systems. In its purest form, it amounts to finding the most economical generation dispatch that meets customer demands and satisfies operational and safety constraints. AC-OPF has also other variants (depending on how the market is organized) and typically include security constraints to ensure reliability under various types of contingencies. AC-OPF problem is a non-convex nonlinear optimization problem [1] which has proven to be NP-hard even if the network is as simple as a tree network [2]. In practice, finding an AC-feasible point without a prior solution has been characterized as “maddeningly difficult” [3].

In recent years, the convexification of AC-OPF has attracted significant amount of interest. This line of research includes the Second-Order Cone (SOC) relaxation [4], the Semi-Definite Programming (SDP) relaxation [5], [6], and the Quadratic Convex (QC) relaxation [1]. These relaxation models can be solved to global optimal by interior-point methods (e.g. IPOPT [7]) in polynomial time, producing a lower bound to the original problem in reasonable amount of time. Solutions from these relaxation methods can also be used as a starting point for the load flow study to recover an AC-feasible solution. Interestingly, Lavaei and Low [6] has shown that, for many of the standard test cases at the time, the SDP relaxation had a zero duality gap and that the optimal solution could be recovered. Subsequent research (e.g., [1], [8]–[10]) has confirmed that these above-mentioned relaxations almost always have small optimality gaps (i.e., the distance between a primal solution and the relaxation bound) on larger collection of test cases.

T.W.K. Mak, L. Shi, and P. Van Hentenryck are with Department of Industrial & Operations Engineering, University of Michigan, 1205 Beal Ave., Ann Arbor, MI 48109, USA {wmak, lynshi, pvanhent}@umich.edu

This paper originated as an attempt to generate hard OPF test cases derived from real networks in the context of the ARPA-E Grid Data project [11]. It considers an interesting part of the French network (called MSR) and investigates when OPF instances have large optimality gaps, which typically indicate that they are hard to solve optimally (or to prove optimality). The main methodology of the paper is to increase the loads in the system uniformly and to understand the resulting impact on the optimal generator dispatches and the optimality gaps. The paper also studies the effect of relaxing some of the generation and voltage constraints, as well as the impact of current limits.

The main outcome of this paper is to show the existence of realistic test cases over a real transmission network that exhibit significant optimality gaps. In addition, the paper shows these optimality gaps exhibit interesting phase transitions and bifurcation points. It was expected that the objective of primal solution and relaxations would start bifurcating as the loads increase and the network becomes congested. However, the experimental results exhibit other bifurcation points and some complex phase transitions. In particular, AC-OPF instances with large optimality gaps may occur even when the network is far from its congestion point. These results have been reproduced on other networks, indicating that these phase transitions are not an artifact of the test case discussed in this paper.

This rest of this paper describes the methodology and experimental results in detail and summarizes the results of more than 6,000 OPF studies with various load profiles, voltage feasibility regions, and generation capabilities. Although the paper does not present results for Security-Constrained OPFs [12], the underlying network being tested is N-1 reliable. Our results would be able to extend naturally to the setting with security constraints.

### II. BACKGROUND

This section introduces the notations and background material. The notations are summarized in Table I. We use complex notations for simplicity as in [1].

#### A. AC Power Flow

Kirchhoffs Current Law (KCL) captures current conservation at a bus  $n \in N$

$$\sum_{g \in G(n)} I_n^g - \sum_{l \in O(n)} I_n^l = \sum_{(n,m): m \in N(n)} I_{nm} \quad (1)$$

Ohm’s Law specifies the current through a line

$$I_{nm} = y_{nm}(V_n - V_m), \quad (2)$$

TABLE I  
NOMENCLATURE

Power network $\mathcal{P} = \langle N, L, G, O \rangle$	
$N$	Set of buses
$N(n) \subseteq N$	Neighboring buses of bus $n$
$L^+ \subseteq N \times N$	Set of transmission lines/transformers $(n, m)$
$L^- \subseteq N \times N$	Reversed set of $L^+$ : $\{(m, n) : (n, m) \in L^+\}$
$L = L^+ \cup L^-$	Set of lines including the original and reversed lines
$G$	Set of generators
$G(n) \subseteq G$	Set of generators at bus $n$
$O$	Set of demands/loads
$O(n) \subseteq O$	Set of demands at bus $n$
$S_n, p_n, q_n$	Complex/active/reactive power at bus $n$
$S_{nm}, p_{nm}, q_{nm}$	Complex/active/reactive power flow from bus $n$ to $m$
$z_{nm}, r_{nm}, x_{nm}$	Impedance/resistance/reactance for line $(n, m)$
$y_{nm}, g^{nm}, b^{nm}$	Admittance/conductance/susceptance for line $(n, m)$
$y_n^s, g_n^s, b_n^s$	Admittance/conductance/susceptance of shunts at bus $n$
$y_{nm}^c, g_{nm}^c, b_{nm}^c$	Admittance/conductance/susceptance of charge at line $(n, m)$
$V_n, I_n$	Complex voltage current at bus $n$
$ V_n /\angle\theta_n$	Voltage magnitude & phase angle at bus $n$
$Tr_{nm}$	Transformer off-nominal turns ratio for transformer $(n, m)$
$\phi_{nm}$	Transformer phase shift for transformer $(n, m)$
$S_n^l, p_n^l, q_n^l$	Complex/active/reactive loads at bus $n$
$S_n^g, p_n^g, q_n^g$	Complex/active/reactive generations at bus $n$
$I_n^g, I_n^l$	Complex current from generations/loads at bus $n$
$I_{nm}$	Complex current flow from bus $n$ to $m$
$\bar{v}, \underline{v}$	Upper/lower limits of quantity $v$
$v^*,  v $	Complex conjugate/magnitude of a complex quantity $v$
$Re(v), Img(v)$	Real/Imaginary part of a complex quantity $v$

and the definition of AC power is given by

$$S_{nm} = p_{nm} + iq_{nm} = V_n(I_{nm})^*. \quad (3)$$

Combining (1)-(3) produces the AC power flow equations:

$$\sum_{g \in G(n)} S_n^g - \sum_{l \in O(n)} S_n^l = \sum_{(n,m):m \in N(n)} S_{nm}, \text{ where} \quad (4)$$

$$S_{nm} = y_{nm}^* V_n V_m^* - y_{nm}^* V_n V_m^* \quad (5)$$

These equations are non-convex and nonlinear and are essential building blocks for many applications in power systems. For implementation purposes, these complex variables (and the equations) are rewritten in terms of real numbers using either the rectangular form (e.g., decomposing  $S_{nm}$  into  $p_{nm}$  and  $q_{nm}$ ), the polar form (e.g., decomposing  $V_n$  into  $|V|$  and  $\theta_n$ ), or a hybrid form.

### B. Optimal Power Flow

Model 1 presents the AC Optimal Power Flow problem (AC-OPF). Constraints (C.1), (C.2), (C.3), and (C.4) implement the voltage (magnitude) bounds, generation limits, line thermal limits, and phase angle difference limits respectively. Constraints (C.5) and (C.6) implement the AC power flow equation. The objective (O.1) sums the generation costs  $c()$  for all the generators.

### C. The SDP, SOCP, and QC Relaxations

The non-convexities in Model 1 stem solely from the voltage products  $(V_n V_m^*)$ . They can be isolated [1], [4], [13]–[15] by introducing  $W$  variables defined as

$$W_{nm} = V_n V_m^* \quad (6)$$

The SDP relaxation [5] reformulates Model 1 by using the  $W_{nm}$  variables and relax equations (6) by imposing that the matrix of  $W$  variable be positive semi-definite (see Model 2).

## Model 1 The AC-OPF Formulation.

### Inputs:

$\mathcal{P} = \langle N, L, G, O \rangle$  Power network input

### Variables:

$V_n, \forall n \in N$  Voltage variables  
 $S_n^g, \forall n \in G$  Power dispatch variables  
 $S_{nm}, \forall (n, m) \in L$  Power flow variables

### Minimize

$$\sum_{n \in G} c(n, Re(S_n^g)) \quad (O.1)$$

### Subject to:

$$|V_n| \leq |V_n| \leq \overline{|V_n|} \quad \forall n \in N \quad (C.1)$$

$$\underline{S_n^g} \leq S_n^g \leq \overline{S_n^g} \quad \forall n \in G \quad (C.2)$$

$$|S_{nm}| \leq \overline{S_{nm}} \quad \forall (n, m) \in L \quad (C.3)$$

$$-\overline{\theta_{nm}} \leq \angle(V_n V_m^*) \leq \overline{\theta_{nm}} \quad \forall (n, m) \in L \quad (C.4)$$

$\forall n \in N$ :

$$\sum_{g \in G(n)} S_n^g - \sum_{l \in O(n)} S_n^l = \sum_{(n,m):m \in N(n)} S_{nm} \quad (C.5)$$

$$S_{nm} = y_{nm}^* V_n V_m^* - y_{nm}^* V_n V_m^* \quad \forall (n, m) \in L \quad (C.6)$$

## Model 2 SDP-OPF: W-variable formulation

### Inputs:

$\mathcal{P} = \langle N, L, G, O \rangle$  Power network input

### Variables:

$W_{nm}, \forall n, m \in N$  W-variables  
 $S_n^g, \forall n \in G$  Power dispatch variables

### Minimize

(O.1)

### Subject to:

(C.2), (C.3), (C.5)

$$|V_n|^2 \leq W_{nn} \leq \overline{|V_n|}^2 \quad \forall n \in N \quad (C.1w)$$

$$\tan(-\overline{\theta_{nm}}) Re(W_{nm}) \leq Img(W_{nm}) \quad \& \quad Img(W_{nm}) \leq \tan(\overline{\theta_{nm}}) Re(W_{nm}) \quad \forall (n, m) \in L^+ \quad (C.4w)$$

$$S_{nm} = y_{nm}^* W_{nn} - y_{nm}^* W_{nm}, \quad \forall (n, m) \in L^+, \quad \&$$

$$S_{mm} = y_{nm}^* W_{mm} - y_{nm}^* W_{nm}^* \quad \forall (n, m) \in L^- \quad (C.6w)$$

$$W \succeq 0 \quad (C.7)$$

Constraints (C.1w), (C.4w), and (C.6w) reformulate constraints (C.1), (C.4), and (C.6) by replacing  $V_n$  with the  $W_{nm}$  variables. Constraint (C.7) enforces the positive semi-definite requirement. Solving the SDP relaxation remains computationally challenging, especially for networks with thousands of variables. This paper only enforces the positive semi-definite constraints on 2 by 2 and 3 by 3 sub-matrices to allow the computational studies tractable, while maintaining strong accuracy [16].

The SOCP relaxation [4] further relaxes the SDP relaxation and relaxes equations (6) with

$$|W_{ij}|^2 \leq W_{ii} W_{jj}. \quad (C.8)$$

The QC relaxation [1] represents voltages  $V_n$  in its polar form  $(|V_n|/\angle\theta_n)$  and reformulate the voltage variables (and their corresponding equations) in Model 1 by directly using the polar form variables  $(|V_n|$  and  $\theta_n)$ . The relaxation uses tight convex envelopes to relax cosine and sine terms and McCormick envelopes [1] for product terms between the voltage magnitude variables  $(|V_n|)$  and the sine/cosine relaxed envelopes.

---

**Model 3** AC-OPF with load scaling
 

---

**Inputs:**

$\mathcal{P} = \langle N, L, G, O \rangle$  Power network input  
 $t, O' \subseteq O$  Load-scaling factor, set of varying loads

**Variables:**

$V_n, \forall n \in N. S_n^g, \forall n \in G. S_{nm}, \forall (n, m) \in L$

**Minimize**

(O.1)

**Subject to:**

(C.1)-(C.4), (C.6)

$\forall n \in N :$

$$\sum_{g \in G(n)} S_n^g - \sum_{l \in O(n)} t^l S_n^l = \sum_{(n,m):m \in N(n)} S_{nm}, \quad (\text{C.9})$$

where  $t^l = \begin{cases} t, & \text{if } l \in O' \\ 1, & \text{otherwise} \end{cases}$

---

**D. Grid Research for Good (GRG) project**

This paper uses test cases from the French transmission network in the context of the Grid Research for Good (GRG) project [11]. The test cases are represented in Node-Breaker (NB) format. The network are composed by substations and transmission lines. Each substation is composed of different voltage levels linked by transformers. Each voltage level contains loads, generators, shunts, and a detailed circuit board containing bus-bars and switches. Since the primary purpose of this study is to investigate the optimality gaps on OPF problems, the test cases are converted using the GRG tools in a Bus-Branch (BB) format using default switching configurations being used in the given snapshot-data. Bus shunts  $y_n^s$ , line charges  $y_{nm}^c$ , and T-model transformers are incorporated into the OPF models according to the GRGv3.0 specification [11] (mainly by modifying (C.5)-(C.7)). All test cases have been validated for accuracy with respect to actual solutions using PowerTools [17] to compute the OPF solutions.

### III. EXPERIMENTAL METHODOLOGY

This section describes the methodology used to produce hard test cases, using Model 1 as a starting point.

**A. Load Scaling**

The experiments consider Model 3 which scales the load by a factor  $t$ . The model receives as input the collection  $O'$  of loads to scale uniformly. When all loads are scaled,  $O' = O$ . The model only replaces (C.5) with (C.9) and the SDP, SOCP, and QC relaxations can be applied directly to solve the SDP-OPF, SOCP-OPF, and QC-OPF problems with scaled loads.

**B. Load Flow Study**

A relaxation typically does not produce a feasible solution to the AC-OPF instance. The experimental results use Model 4 to recover the closest active generation dispatch (using a L2 norm) to the solution  $\hat{p}_n^g$  of a relaxation. Once this solution is recovered, it can be evaluated using Objective (O.1) to obtain the dispatch cost.

---

**Model 4** Load flow study for relaxation methods
 

---

**Inputs:**

$\mathcal{P} = \langle N, L, G, O \rangle$  Power network input  
 $\hat{p}_n^g$  Active generation dispatch from relaxation

**Variables:**

$V_n, \forall n \in N. S_n^g, \forall n \in G. S_{nm}, \forall (n, m) \in L$

**Minimize**

$[Re(S_n^g) - \hat{p}_n^g]^2$

**Subject to:**

(C.1)-(C.4),(C.6),(C.9)

---

TABLE II  
 MAIN METRICS OF THE MSR TEST CASE

Network components		Generator number (fuel type)	
Substation	285	Solar	76
Voltage Level	365	Wind	5
Busbar	706	Thermal	15
Line	452	Hydro	81
Transformer	122	Nuclear	0
Load	594		
Shunt	42		
Switch number (type)		Line Impedance (Ohm)	
Breaker	2166	Resistance (max)	6.98
Wind	2982	Reactance (max)	31.93
		Resistance (avg)	0.88
		Reactance (avg)	3.12

### IV. EXPERIMENTAL EVALUATIONS

This section describes the experimental study on OPF for the MSR test case. The MSR benchmark, obtained in the context of the GRG project [11], represents an interesting subset of the French transmission system and its main metrics are defined in Table II. The benchmark contains the network topology and operations data, but did not come with market/generation costs since OPFs for the European market aim to minimize the distance of the generator dispatches to a given set of target set-points. The experimental results assumes a quadratic cost function for the generator which is tailored to different fuel types: solar, wind, hydro, thermal, and nuclear generators. The quadratic coefficients is zero for the first three types. MSR also contains negative loads, which are used to model boundary conditions, e.g., generation supply or tie-line support from other French regions and connected countries, domestic renewable generations, and/or reactive support devices. In the experiments, they are not consider as proper loads and are treated as constant power injections.

The experimental results summarize optimal power flow solutions for more than 6000 scenarios for various power flow models, load profiles, voltage feasibility regions, and generation capabilities obtained by running Model 3 on the MSR benchmark, and the corresponding load-flow problem for each relaxation. The study originates from the ARPA-E Grid Data program and the desire to obtain hard instances of OPFs. In particular, it focuses on generating OPF test cases where the optimality gaps between the AC model and the relaxations are large. This typically means that global optimization solvers will be challenged to obtain optimal solutions and/or to prove optimality. The optimality gap (in

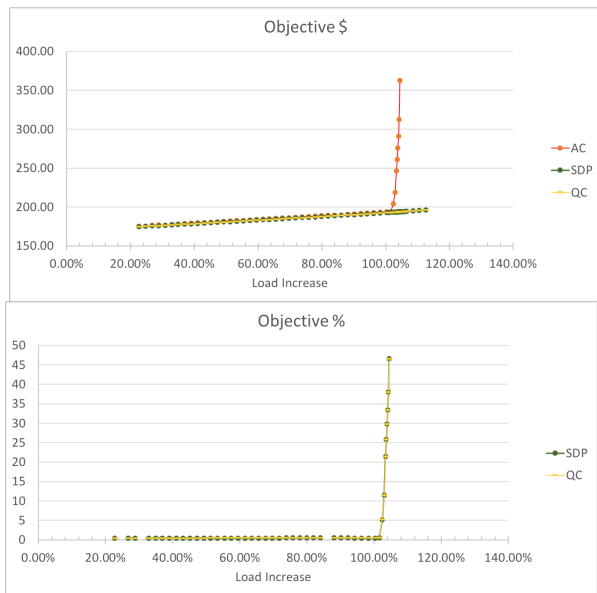


Fig. 1. Objective Costs (top) and Optimality Gaps (bottom) on MSR-5. percentage) is defined as

$$100\% \times \left(1 - \frac{\hat{c}}{c}\right) \quad (7)$$

where  $c$  is the cost obtained by solving the AC-OPF problem with a (locally optimal) non-linear solver and cost  $\hat{c}$  is the cost obtained by solving a relaxation. The study also reports the gap between the primal AC solutions and the load flows applied to the relaxation solutions using (Model 4), a topic which has been largely neglected in the past.

All our models are implemented on PowerTools [17] in the GRG-Tools framework [11]. They are solved using IPOPT [7] solver with MA57 (or MA97 for large instances) linear routines [18]. .

#### A. A Preliminary Experiment

These preliminary study (MSR-5) only increases the 5 loads with the lowest bus voltage magnitudes (in the setpoints provided for MSR). The loads are increased from 20% to 105% (by approx. 2% interval, up to approx. 0.5% when close to transition point). Figure 1 shows the objective costs and optimality gaps for the AC-OPF, QC-OPF, and SDP-OPF model. Since the objective costs for SOCP-OPF are almost always the same as QC-OPF, they are not depicted in the graph for clarity. Figure 1 shows that convex relaxations are extremely accurate (almost zero optimality gap) until the system becomes heavily congested (i.e., when the loads are increased by more than  $> 100\%$ ). At that stage, the objective costs between the AC and the relaxation solutions start bifurcating, exhibiting test cases with large optimality gaps (up to about 50%). At some point, the AC solver no longer converges, while the relaxations continue to produce “lower bounds”. Finally, around the 120% load increase, the relaxations prove infeasibility. Figure 2 depicts the results of the load-flow studies. The load-flow model successfully recovers solutions close to the AC solution but they are approx. 5% away from the AC solutions. This preliminary

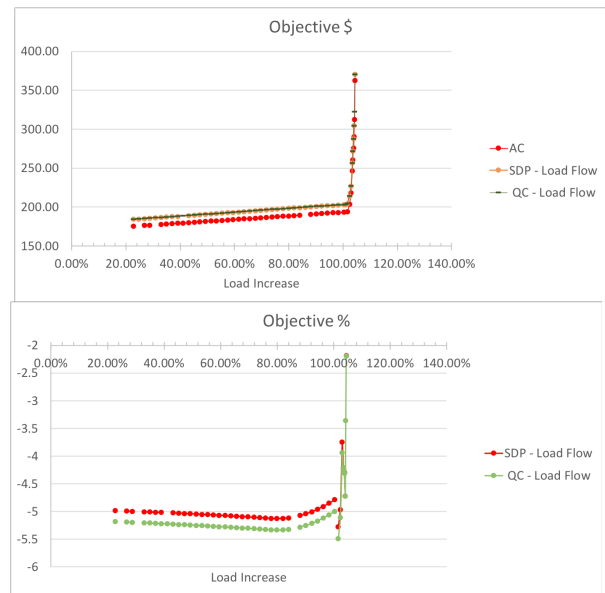


Fig. 2. Objective Costs (top) and Solution Quality (bottom) for the Load-flow study on MSR-5.

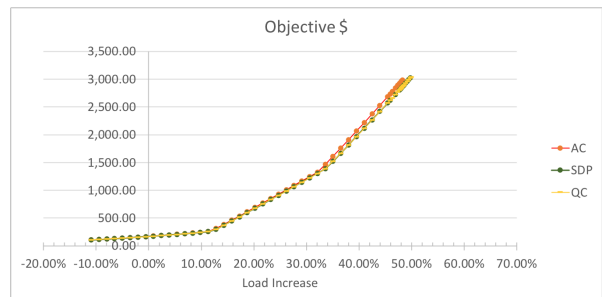


Fig. 3. Objective Costs on the MSR Test Case.

study shows that it is possible to generate hard test cases on real networks, although the test cases proposed in this first study are highly unrealistic.

#### B. Uniform Load Increases

To obtain realistic hard test cases, this second study increases all the loads proportionally. Figure 3 depicts the objective costs for the AC-OPF, QC-OPF, and SDP-OPF models and Figure 4 depicts the load flow results.

These results once again highlight the strength of convex relaxations whose solutions are within 3% of the AC solutions in general. The gap slightly increases when the network becomes really congested but remains below 6%. Figure 4 show the results of the load flows which recover very high-quality solutions. An interesting features of these instances is that the generators systematically hit their upper bounds when loads are increased uniformly. Very few of the remaining constraints were binding, which explains why the convex relaxations were so accurate.

#### C. Relaxing Generation Bounds

To generate more interesting test cases, this third study increases the generator capacity by 200%. Such an increase

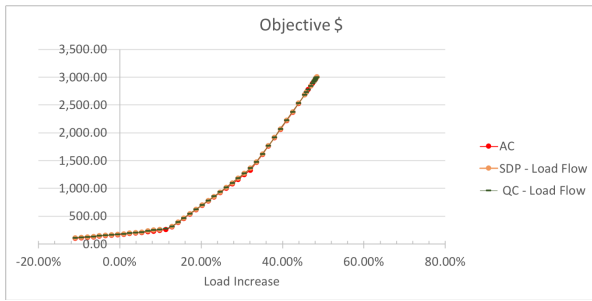


Fig. 4. Load-flow Study on the MSR Test Case.

TABLE III  
CASE 3: OBJECTIVE COST (\$)

Load Inc.	55.98%	56.12%	56.14%	56.29%	56.92%	62.38%	63.94%
AC-OPF	3,366.49	3,499.93	—	—	—	—	—
SOCF	2,356.95	2,371.02	2,372.59	2,388.26	2,451.16	3,009.20	3,169.99
SDP	2,357.97	2,372.05	2,373.62	2,389.30	2,452.22	—	3,171.35
QC	2,356.55	2,370.63	2,372.19	2,387.86	2,450.76	3,008.78	3,169.57

can also be interpreted as the commitment of more generators. The loads are then varied from a 10% decrease up to a maximum of 80% increase. Figure 5 depicts the results for this test case, denoted by MSR-200. The results are particularly interesting. First, Figure 5(top) shows again a bifurcation of the costs of the AC solver and the relaxations, following by the non-convergence of the AC solver (at 57%), and the proof of infeasibility by the relaxation (at about 75%). But the scale of the figure, with the sharp increase in costs, hides a second interesting phenomenon. Indeed, Figure 5(bottom) exhibits another phase transition at around 20% load increase, producing optimality gaps of about 20%. These large optimality gaps disappear at around the 30% load increase before the final increase and bifurcation. A *direct consequence of these results is the existence of realistic test cases over real networks with large optimality gaps.*

Figure 6 shows that it is always possible to recover primal solutions from the relaxations when the AC solver converges and that these recovered solutions are extremely close to the AC solutions. It is tempting to conclude that the AC solution is optimal or close to optimal but further analysis is needed to draw a definite conclusion, since the load flows recover primal solution without being guided by the cost objective.

It is important to understand the cause of this phenomenon. Figure 7 shows that the percentage of buses with tight voltage magnitudes exhibit the same phase transitions as the optimality gaps. Moreover, the load flow solutions have similar shapes for active voltage magnitude constraints as the AC solutions. The relaxations work around the voltage magnitude constraints by “throwing away power” at selected buses in the network. This phenomenon is not present for the current limits as shown in Figure 8 suggesting current limits are not contributing to the large optimality gaps.

#### D. Numerical Issues

Figure 9 reports the CPU time in seconds to solve these models. The load-flow procedure to recover an AC-feasible solution for QC/SDP runs longer when QC/SDP have significant optimality gap. These results, which were

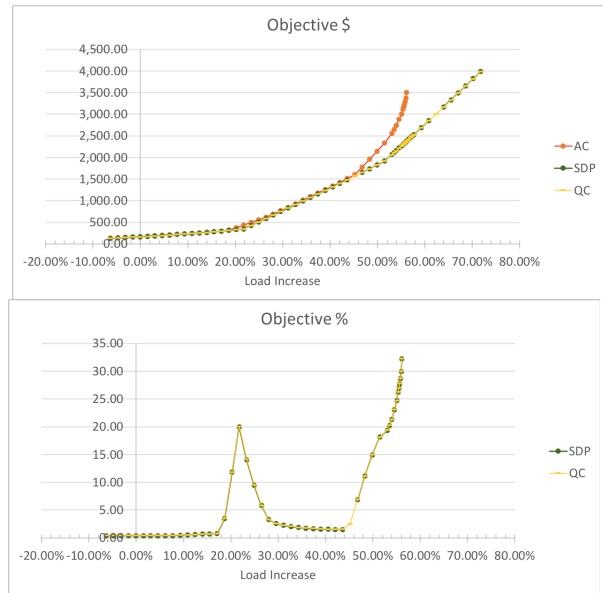


Fig. 5. Objective Costs (top) and Optimality Gaps (bottom) on MSR-200.

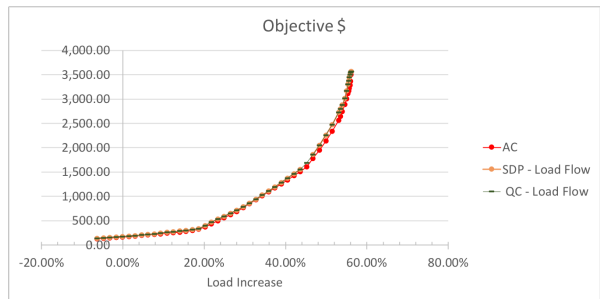


Fig. 6. Load Flow Results on MSR-200.

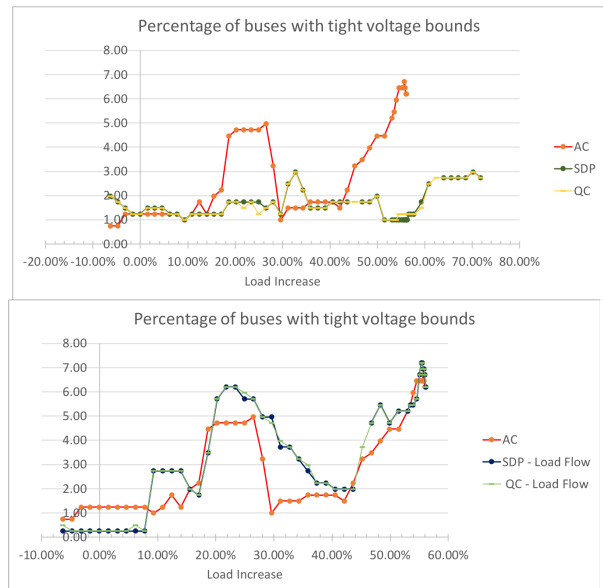


Fig. 7. Percentage of Buses with Active Voltage Magnitude Constraints. Top: AC/QC/SDP-OPF. Bottom: Load Flows.

also confirmed on other test cases, show the existence of realistic test cases over real networks that exhibit some interesting numerical issues and wide variations in execution

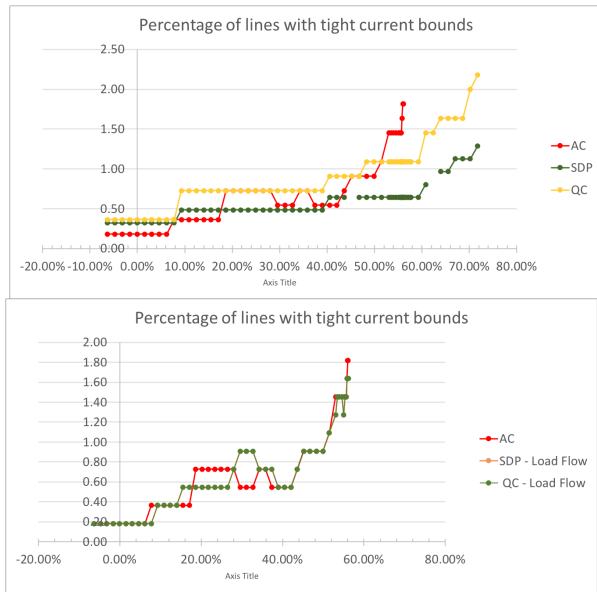


Fig. 8. Percentage of Lines/Transformers with Active Current Flow Limits. Top: AC/QC/SDP-OPF, Bottom: Load Flows.

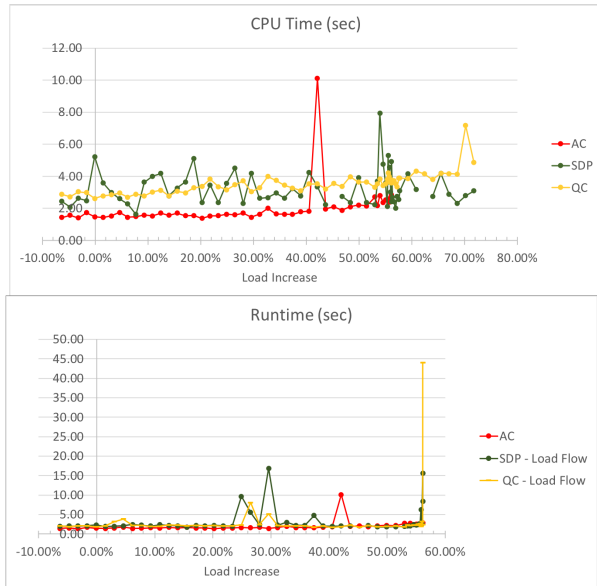


Fig. 9. CPU Runtimes (sec). Top: AC/QC/SDP-OPF, Bottom: Load Flow times, even when the network is not congested.

## V. CONCLUSION

This paper investigated the existence of large optimality gaps in real OPFs. Convex relaxations have been shown to produce highly accurate bounds on OPF problems, despite NP-Hardness results even on a simple star (radial) network. Using a subset of the French transmission Systems, the paper showed that large optimality gaps exist in real-world networks. Indeed, we showed increasing the loads uniformly by 22% produced test cases with optimality gaps of 20%. Most interestingly perhaps, these large optimality gaps occur even when the network is not congested and the loads could be increased much further.

The paper also isolated some interesting phenomena on

the optimality gaps. Close to the congestion point, the test case exhibits a bifurcation of the AC cost and the costs of the relaxations. The AC solver then encounters convergence issues, while the relaxations still produce “lower bounds”, before finally proving infeasibility.

In addition, the test case also exhibits large optimality gaps even if it is not congested, with regions of large gaps followed by regions of small gaps. These phase transitions were explained by similar transitions in the percentage of tight voltage bounds in the AC solution. The relaxations in contrast did not exhibit the same behavior. These phase transitions were not present in the current limit plot. Similar behavior were observed on other large-scale networks and will be presented in our future work.

## VI. ACKNOWLEDGMENTS

This research is supported by ARPA-E grant 1357-1530 “High Fidelity, Year Long Power Network Data Sets for Replicable Power System Research.

## REFERENCES

- [1] C. Coffrin, H. Hijazi, and P. Van Hentenryck, “The QC relaxation: A theoretical and computational study on optimal power flow,” *IEEE Transactions on Power Systems*, vol. 31, no. 4, pp. 3008–3018, July 2016.
- [2] K. Lehmann, A. Grastien, and P. Van Hentenryck, “Ac-feasibility on tree networks is np-hard,” *IEEE Transactions on Power Systems*, vol. 31, no. 1, pp. 798–801, Jan 2016.
- [3] T. J. Overbye, X. Cheng, and Y. Sun, “A comparison of the AC and DC power flow models for LMP calculations,” in *Proceedings of the 37th Annual Hawaii International Conference on System Sciences*, 2004.
- [4] R. A. Jabr, “Radial distribution load flow using conic programming,” *IEEE Transactions on Power Systems*, vol. 21, no. 3, pp. 1458–1459, Aug 2006.
- [5] X. Bai, H. Wei, K. Fujisawa, and Y. Wang, “Semidefinite programming for optimal power flow problems,” *International Journal of Electrical Power & Energy Systems*, vol. 30, no. 6, pp. 383 – 392, 2008.
- [6] J. Lavaei and S. H. Low, “Zero duality gap in optimal power flow problem,” *IEEE Transactions on Power Systems*, vol. 27, no. 1, pp. 92–107, Feb 2012.
- [7] A. Wächter and L. T. Biegler, “On the implementation of an interior-point filter line-search algorithm for large-scale nonlinear programming,” *Mathematical Programming*, vol. 106, no. 1, pp. 25–57, 2006.
- [8] C. Coffrin, H. L. Hijazi, and P. Van Hentenryck, “Strengthening convex relaxations with bound tightening for power network optimization,” in *Principles and Practice of Constraint Programming*, 2015, pp. 39–57.
- [9] H. Hijazi, C. Coffrin, and P. V. Hentenryck, “Convex quadratic relaxations for mixed-integer nonlinear programs in power systems,” *Mathematical Programming Computation*, vol. 9, no. 3, pp. 321–367, Sep 2017.
- [10] C. Coffrin, H. L. Hijazi, and P. Van Hentenryck, “Strengthening the sdp relaxation of ac power flows with convex envelopes, bound tightening, and valid inequalities,” *IEEE Transactions on Power Systems*, vol. 32, no. 5, pp. 3549–3558, 2017.
- [11] “Grid Research for Good,” Grid Research for Good: <https://gdg.engin.umich.edu/>, 2018.
- [12] A. Monticelli, M. V. F. Pereira, and S. Granville, “Security-constrained optimal power flow with post-contingency corrective rescheduling,” *IEEE Transactions on Power Systems*, vol. 2, no. 1, pp. 175–180, Feb 1987.
- [13] A. Gmez Expósito and E. Romero Ramos, “Reliable load flow technique for radial distribution networks,” *IEEE Transactions on Power Systems*, vol. 14, no. 3, pp. 1063–1069, Aug 1999.
- [14] R. A. Jabr, “Optimal power flow using an extended conic quadratic formulation,” *IEEE Transactions on Power Systems*, vol. 23, no. 3, pp. 1000–1008, Aug 2008.
- [15] S. Sojoudi and J. Lavaei, “Physics of power networks makes hard optimization problems easy to solve,” in *2012 IEEE Power and Energy Society General Meeting*, July 2012, pp. 1–8.

- [16] H. Hijazi, C. Coffrin, and P. V. Hentenryck, "Polynomial sdp cuts for optimal power flow," in *2016 Power Systems Computation Conference (PSCC)*, June 2016, pp. 1–7.
- [17] "Powertools," Powertools: <http://hhijazi.github.io/PowerTools/>, 2017.
- [18] "A collection of Fortran codes for large scale scientific computation," <http://www.hsl.rl.ac.uk/>, 2016.